RSC Advances

PAPER

View Article Online
View Journal | View Issue

Cite this: *RSC Adv.*, 2025, **15**, 44749

Synthesis and characterization of novel quinazolinone-based azo disperse dyes: molecular docking, ADMET, *in vitro*, and dyeing performance on polyester fabric

Ahmed A. Noser, *[ab] Abdulrahman A. Almehizia,[c] Mohamed A. Al-Omar,[c] Faris Ibrahim Alrayes,[c] Mohanad Mousa Kareem,[d] Khadra B. Alomari,[e] Maha Ali Aljowni[f] and Seham A. Ibrahim[a]

A series of new azo quinazolinone disperse dyes was synthesized and characterized using various spectroscopic techniques. The synthetic azo dyes were applied to polyester fabrics, and their multifunctional properties, such as fastness, color assessment, dye exhaustion, fixation, pH effect, color strength, dyeing time, and dye concentration, were studied and yielded reasonable results, indicating the dyes' effectiveness in dyeing polyester. Additionally, the UV protection factor of the dyes was evaluated; results showed that these dyes provide excellent UV protection. The mode of action of these compounds was also examined both *in silico* through molecular docking and *in vitro* to assess their potential antimicrobial properties. Furthermore, ADMET pharmacokinetics were analyzed. The experimental data aligned with the molecular docking findings, which indicated that compound **5b** inhibited bacterial DNA gyrase with a binding score of −10.32 kcal mol^{-1}. Based on these results, it can be concluded that the newly synthesized dyes have strong potential in the textile dyeing industry and may be further developed.

Received 6th October 2025
Accepted 9th November 2025

DOI: 10.1039/d5ra07614e

rsc.li/rsc-advances

Introduction

A vital medical requirement for developing new types of antibacterial agents has emerged due to the rise of drug resistance.[1,2] The need to create original antibiotics to fight resistant bacteria is increasing as drug-resistant strains become more prevalent. Nitrogen-containing heterocycles like quinazolinones have attracted significant interest because of their diverse and widely used biopharmaceutical properties.[3–6] Quinazolines are recognized as important compounds for synthesizing numerous molecules with physiological and pharmacological uses. They serve as building blocks for about 200 biologically active, naturally occurring alkaloids. Key properties such as anticancer, antibacterial, anti-inflammatory, antifungal, anti-HIV, anticonvulsant, and anti-analgesic effects have been established by various substituted quinazolines and quinazolinones.[7–13] Azo dyes, which are a crucial class of colorants, are among the most common dyes for fiber dyeing due to their extensive applications in science and industry.[14–16] They are the most widely used synthetic dyes because of their ease of preparation and broad industrial uses, including advanced applications in organic synthesis, paper printing, cosmetics, plastics, and textile dyeing.[17–19] A wide range of pharmacological and biological properties of azo dyes with heterocycles have been explored.[20,21] The heterocyclic components of azo dyes are essential for developing their pharmacological and therapeutic effects, such as antibacterial,[22] antioxidant,[23] anti-inflammatory,[24] and antitumor[25] activities.

Furthermore, synthetic azo dyes are better than natural dyes in the dyestuff industry due to their price, ease of synthesis, stability, and color variety. Azo dyes with a heterocyclic moiety are noted for their coloring power, tinctorial strength, fastness, and thermal stability. Additionally, the cell bathochromic impact of azo dyes is stronger than that of dyes with simple aromatic systems.[26–29] The majority of disperse dyes are azo dyes, which have a high color gamut and can yield an extensive range of molecular combinations by adjusting the diazo and coupling components.[30] Because of the brilliant fastness

[a]*Chemistry Department, Faculty of Science, Tanta University, Tanta 31527, Egypt*
[b]*Al-Amal College for Specialized Medical Sciences, Department of Pharmacy, Karbala, Iraq*
[c]*Drug Exploration and Development Chair (DEDC), Department of Pharmaceutical Chemistry, College of Pharmacy, King Saud University, P. O. Box 2457, Riyadh 11451, Saudi Arabia*
[d]*Department of Chemistry, College of Science, University of Babylon, P. O. box 51002, Hilla, Iraq*
[e]*Department of Physical Sciences, Chemistry Division, Jazan University, P. O. Box 114, 45142, Jazan, Saudi Arabia*
[f]*Department of Chemistry, Faculty of Science, University of Tabuk, Tabuk 71491, Saudi Arabia*

properties, wide color range, and brilliance,[31] disperse azo dyes are particularly well-liked for dyeing polyester fabrics.[32] The synthesis of novel dispersible dyes with enhanced qualities for dyeing polyester has progressed significantly in recent years.

Numerous research teams have fashioned disperse dyes with altered molecular structures to advance polyesters' strength, color fastness, and intensity. Innovative disperse dyes that have confirmed outstanding compatibility and affinity for dyeing polyester fabrics include dyes based on quinazolinone[33] and dyes with long naphthalene ring conjugations.[34] Application studies show that these structural alterations have resulted in disperse dyes with outstanding heat stability, migration resistance, brilliant hues, and high tinctorial strength. In order to meet the obligatory color strength (K/S) and avoid dye waste from low dye fixation, there is a rising tendency to synthesize and use new synthetic colorant analogs to progress dye exhaustion.[35] A multitude of compounds derived from quinazolinone, Schiff base, and azo derivatives have been permitted for use as pharmaceuticals (Fig. 1).[36–38]

Hydroxyl (–OH) and amino (–NH_2) groups are frequently found in dyes, especially in azo and heterocyclic dyes. Because they can affect the dye's solubility, reactivity, and final color, these functional groups are essential to their characteristics. Although both groups can donate electrons, they do so in different ways. In general, amino groups are more effective at doing so than hydroxyl groups. Deeper or shifted colors in the visible spectrum are frequently the consequence of a bathochromic shift (red shift) of dye absorption caused by this increased electron donation. Furthermore, hydroxyl groups affect substrate affinity and dye solubility. While amino groups may increase affinity fibers, because of their polarity and capacity to form ionic interactions, hydroxyl groups can increase water solubility and form hydrogen bonds, both of which are essential for some dyeing processes.[39–44]

This work aims to explore six dispersed dyes with dissimilar functional groups (number and positions) and to assess the synthetic azo dyes' dyeing capabilities on polyester fibers. Additionally, a thorough investigation was conducted into the

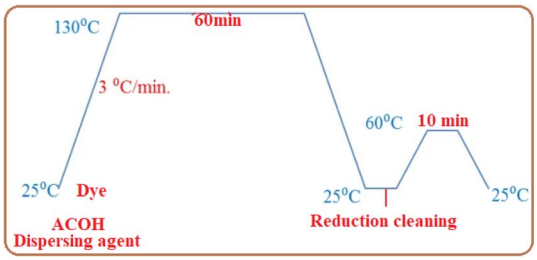

Fig. 2 Polyester fabric one bath dyeing profile.

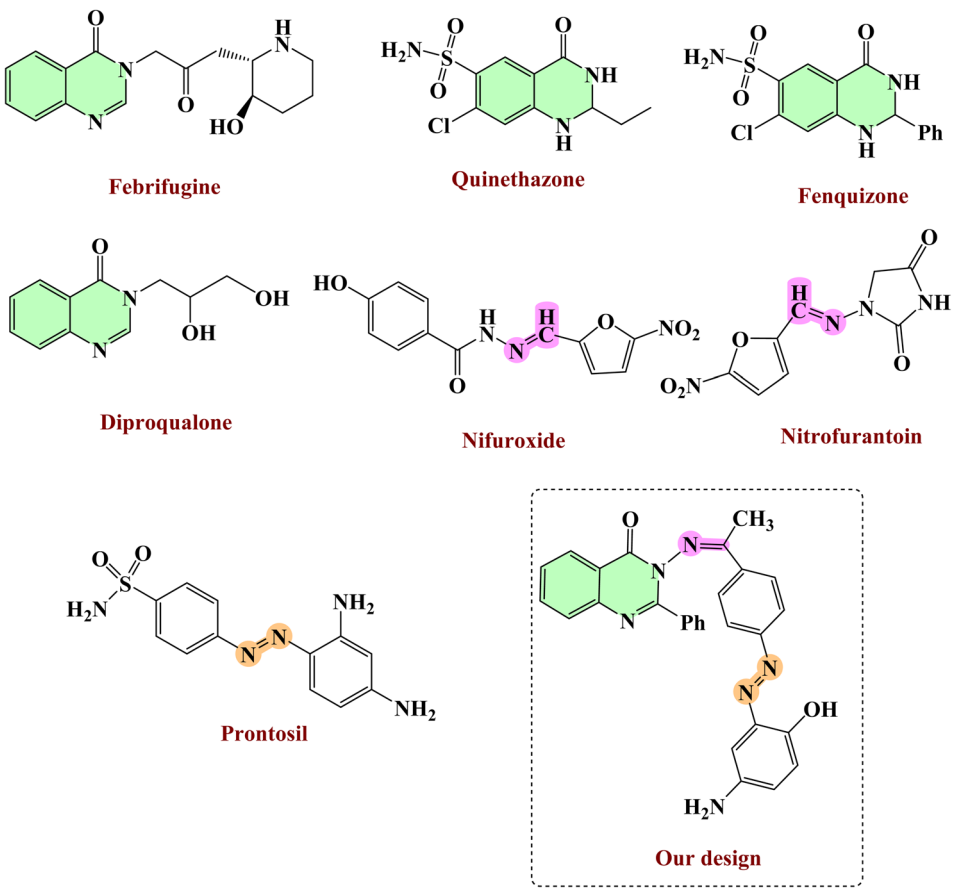

Fig. 1 Pharmaceutical drugs owning the quinazolines and quinazolinones structure.

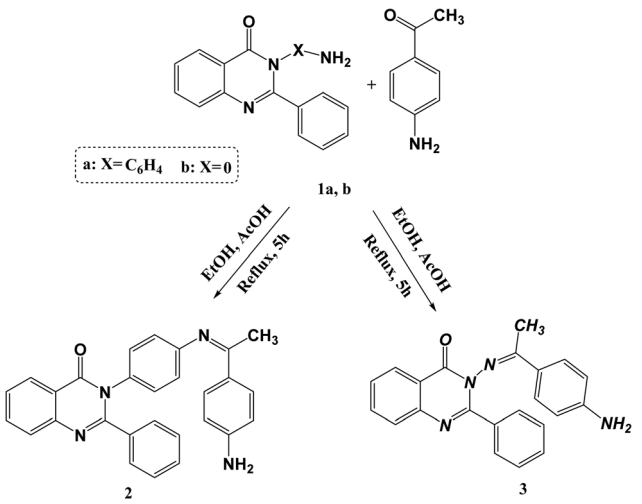

Scheme 1 Synthesis of compounds 2, 3.

multifunctional properties, which included color representation, fastness properties of the dyed samples, and the color's position in L^*, a^*, and b^* (CIELAB coordinates). Furthermore, the color strength characteristics (K/S) and dyeing specifications, including temperature, dye concentration, dyeing time, and pH, were inspected, along with the fixation (% F) and dye exhaustion (% E). Also, the dyed fabrics' UV protection factor was examined. In addition, the antibacterial efficacy of dyes against diverse bacteria and fungi was tested both *in silico* and *in vitro*.

Experimental

Chemicals and instrumentation

Chemicals and instrumentation are designated in the SI file (Section S1).

Organic synthesis

Synthesis of compounds 2 and 3. Compounds **2** and **3** were prepared according to previously described methods.[21]

Synthesis of compounds 4a–c and 5a–c. A cooled solution of compounds **2** or **3** (13.7 mmol) in concentrated hydrochloric acid was mixed with a cooled sodium nitrite solution in water (0.9 g, 12.7 mmol). A cooled solution of various couplers (8.5

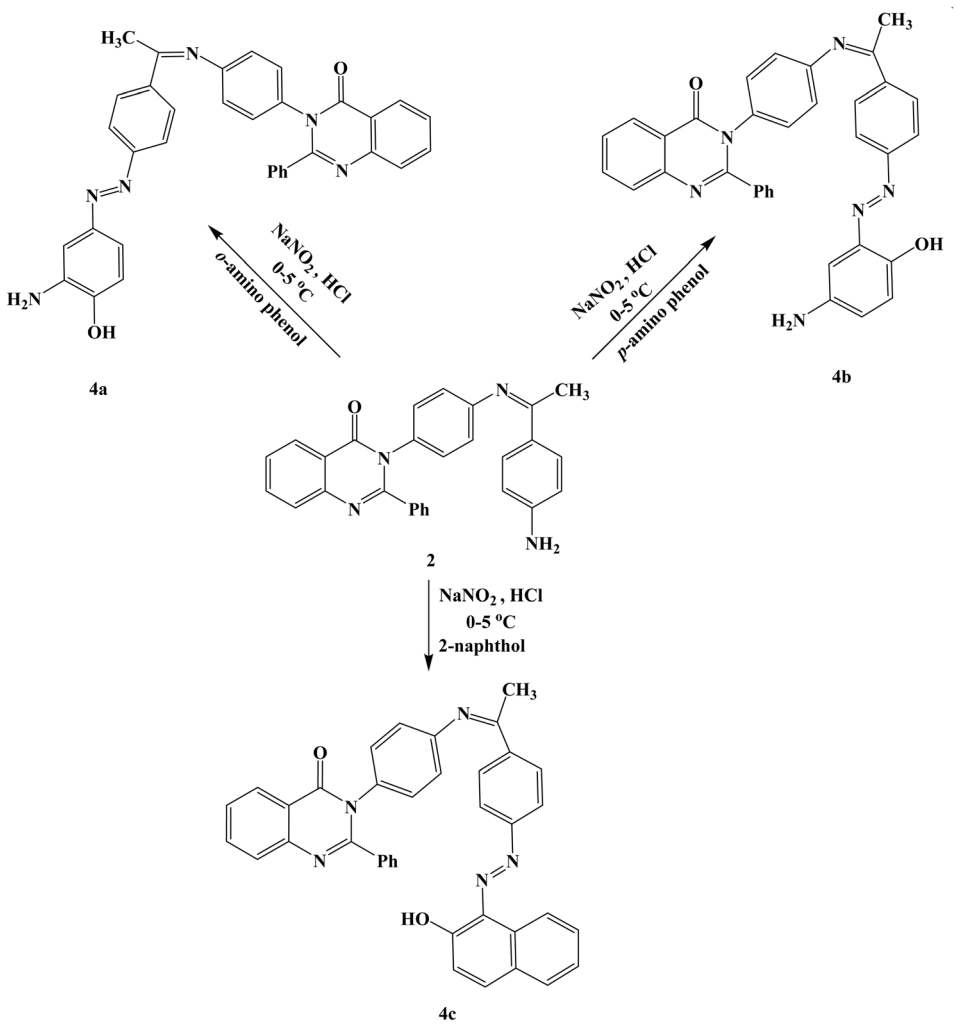

Scheme 2 Synthesis of compounds 4a–c.

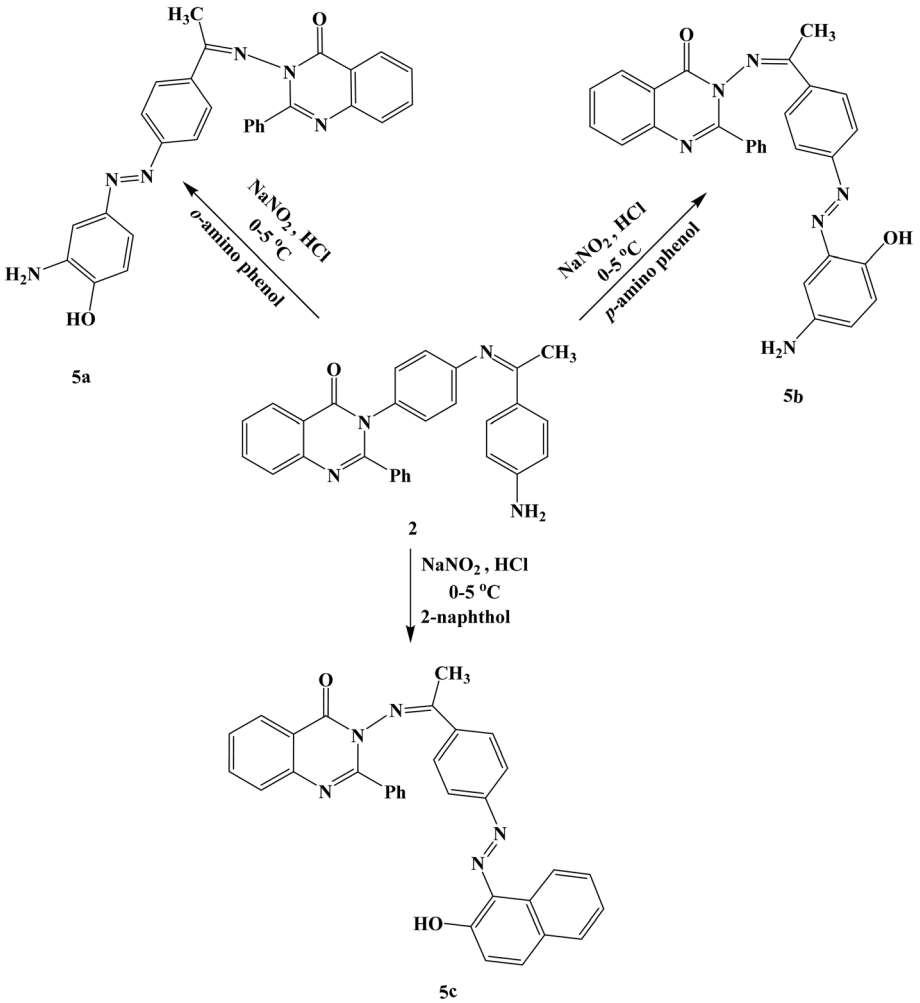

Scheme 3 Synthesis of compounds **5a–c**.

mmol) diluted in 15 mL of 10% NaOH was then mixed with the diazonium salt. After filtering, the product was dried.

3-(4-((((Z)-1-(4-((E)-(3-Amino-4-hydroxyphenyl)diazenyl)phenyl) ethylidene)amino)phenyl)-2-phenylquinazolin-4(3H)-one ***(4a)***. Yield, 91%; m.p.: 170–172 °C; FT-IR (KBr, ν_{max}, cm^{-1}): 3360 (NH_2), 3216 (OH), 3057 (CH-arom), 2973 (CH-aliph), 1755 (CO), 1615 (C=N), 1555 (N=N); ^{1}H-NMR (400 MHz, DMSO-d_6, δ, ppm): 8.69 (s, 1H, NH_2), 7.17–7.93 (m, 20H, Ar-H), 6.55 (s, 1H, OH), 2.34 (s, 3H, CH_3); ^{13}C NMR (100 MHz, DMSO-d_6, δ, ppm): 170.52 (C=N Schiff base), 165.26 (C=N quinazolinone), 164.13 (C=O quinazolinone), 117.11–148.52 (Ar-C), 22.25 (CH_3); MS (EI) m/z [M^+] calcd for $C_{34}H_{26}N_6O_2$: 550.62, found: 550.81; anal. calcd for $C_{34}H_{26}N_6O_2$ (550.62): C, 74.17%; H, 4.76%; N, 15.26%. Found: C, 74.03%; H, 4.63%; N, 15.16%.

3-(4-((((Z)-1-(4-((E)-(5-Amino-2-hydroxyphenyl)diazenyl)phenyl) ethylidene)amino)phenyl)-2-phenylquinazolin-4(3H)-one ***(4b)***. Yield, 93%; m.p.: 155–157 °C; FT-IR (KBr, ν_{max}, cm^{-1}): 3345 (NH_2), 3218 (OH), 3062 (CH-arom), 2955 (CH-aliph), 1735 (CO), 1654 (C=N), 1525 (N=N); ^{1}H-NMR (400 MHz, DMSO-d_6, δ, ppm): 8.69 (s, 1H, NH_2), 7.55–7.93 (m, 20H, Ar-H), 6.49 (s, 1H,

Table 1 Absorption spectra of dyes **4a–c**

Compound no.	λ_{max} (nm) (benzene)	ε	λ_{max} (nm) (EtOH)	ε	λ_{max} (nm) (DMF)	ε
4a	373	884	390	1034	419	1733
4b	379	945	398	1255	424	1976
4c	389	1767	410	2010	431	2410
5a	373	644	388	1124	415	1114
5b	377	656	395	1718	420	1135
5c	390	1734	406	1889	430	2365

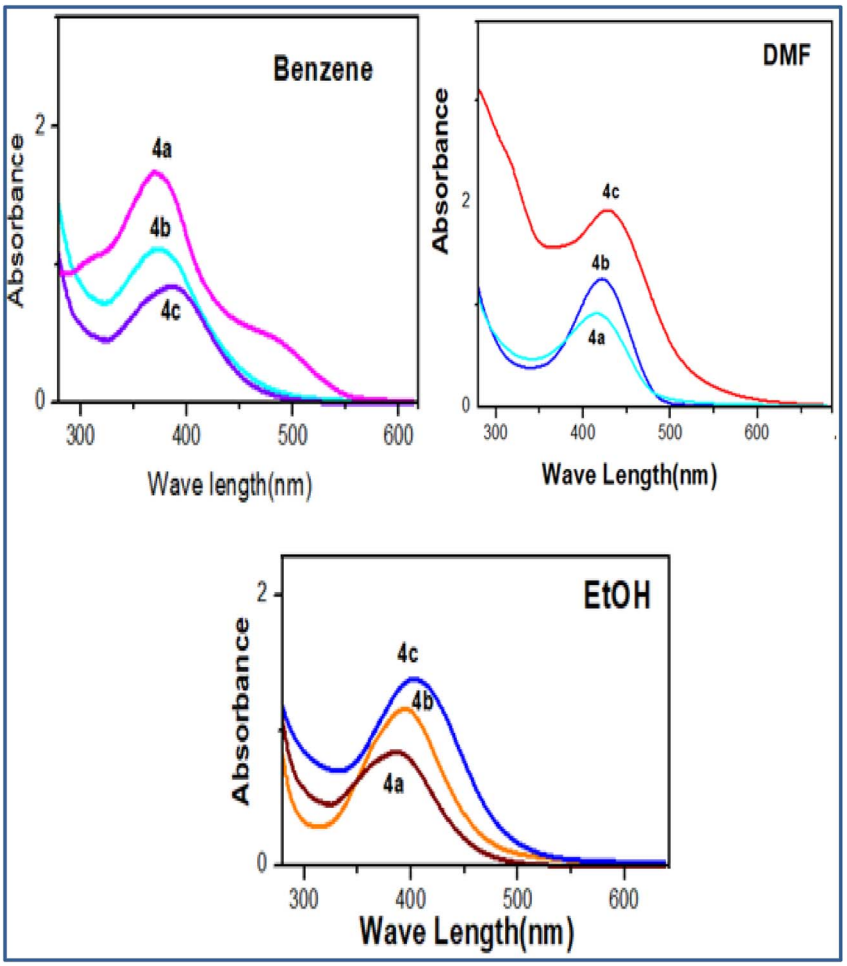

Fig. 3 Dyes **4a–c** absorption spectra in different solvents.

OH), 2.34 (s, 3H, CH_3); ^{13}C NMR (100 MHz, DMSO-d_6, δ, ppm): 170.52 (C=N Schiff base), 165.26 (C=N quinazolinone), 164.79 (C=O quinazolinone), 117.12–155.84 (Ar-C), 23.89 (CH_3); MS (EI) m/z [$M^+ - 1$] calcd for $C_{34}H_{26}N_6O_2$: 550.62, found: 549.57; anal. calcd for $C_{34}H_{26}N_6O_2$ (550.62): C, 74.17%; H, 4.76%; N, 15.26%. Found: C, 74.03%; H, 4.63%; N, 15.16%.

3-(4-(((Z)-1-(4-((E)-(2-Hydroxynaphthalen-1-yl)diazenyl)phenyl) ethylidene)amino)phenyl)-2-phenylquinazolin-4(3H)-one (***4c***). Yield, 92%; m.p.: 118–121 °C; FT-IR (KBr, ν_{max}, cm^{-1}): 3215 (OH), 3055 (CH-arom), 2944 (CH-aliph), 1714 (CO), 1605 (C=N), 1575 (N=N); ^{1}H-NMR (400 MHz, DMSO-d_6, δ, ppm): 6.75–8.12 (m, 23H, Ar-H), 4.99 (s, 1H, OH), 2.43 (s, 3H, CH_3); ^{13}C NMR (100 MHz, DMSO-d_6, δ, ppm): 160.45 (C=N Schiff base), 153.95 (C=O quinazolinone), 149.11 (C=N quinazolinone), 115.51–141.20 (Ar-C), 21.47 (CH_3); MS (EI) m/z [$M^+ + 2$] calcd for $C_{38}H_{27}N_5O_2$: 585.67, found: 585.24; anal. calcd for $C_{38}H_{27}N_5O_2$ (585.67): C, 77.93%; H, 4.65%; N, 11.96%. Found: C, 77.63%; H, 4.37%; N, 11.78%.

3-(((Z)-1-(4-((E)-(3-Amino-4-hydroxyphenyl)diazenyl)phenyl)ethylidene)amino)-2-phenylquinazolin-4(3H)-one (***5a***). Yield, 91%; m.p.: 100–102 °C; FT-IR (KBr, ν_{max}, cm^{-1}): 3325 (NH_2), 3215 (OH), 3045 (CH-arom), 2922 (CH-aliph), 1744 (CO), 1622 (C=N), 1553 (N=N); ^{1}H-NMR (400 MHz, DMSO-d_6, δ, ppm): 10.82 (s, 2H, NH_2), 6.69–7.93 (m, 16H, Ar-H), 4.96 (s, 1H, OH), 2.19 (s, 3H, CH_3); ^{13}C NMR (100 MHz, DMSO-d_6, δ, ppm): 153.41 (C=N Schiff base), 150.12 (C=O quinazolinone), 147.47 (C=N quinazolinone), 119.89–146.21 (Ar-C), 20.02 (CH_3); MS (EI) m/z [$M^+ - 1$] calcd for $C_{28}H_{22}N_6O_2$: 474.52, found: 473.94; anal. calcd for $C_{28}H_{22}N_6O_2$ (474.52): C, 70.87%; H, 4.67%; N, 17.71%. Found: C, 70.67%; H, 4.57%; N, 17.53%.

3-(((Z)-1-(4-((E)-(5-Amino-2-hydroxyphenyl)diazenyl)phenyl)ethylidene)amino)-2-phenylquinazolin-4(3H)-one (***5b***). Yield 93%; m.p.: 90–92 °C; FT-IR (KBr, ν_{max}, cm^{-1}): 3360 (NH_2), 3254 (OH), 3077 (CH-arom), 2963 (CH-aliph), 1725 (CO), 1590 (C=N), 1552 (N=N); ^{1}H-NMR (400 MHz, DMSO-d_6, δ, ppm): 10.26 (s, 2H, NH_2), 6.72–8.22 (m, 16H, Ar-H), 6.55 (s, 1H, OH), 2.37 (s, 3H, CH_3); ^{13}C NMR (100 MHz, DMSO-d_6, δ, ppm): 166.42 (C=N Schiff base), 159.96 (C=N quinazolinone), 152.83 (C=O quinazolinone), 114.86–150.92 (Ar-C), 26.22 (CH_3); MS (EI) m/z [$M^+ + 2$] calcd for $C_{28}H_{22}N_6O_2$: 474.52, found: 474.91; anal. calcd for $C_{28}H_{22}N_6O_2$ (474.52): C, 70.87%; H, 4.67%; N, 17.71%. Found: C, 70.67%; H, 4.57%; N, 17.53%.

3-(((Z)-1-(4-((E)-(2-Hydroxynaphthalen-1-yl)diazenyl)phenyl)ethylidene)amino)-2-phenylquinazolin-4(3H)-one (***5c***). Yield, 92%; m.p.: 95–97 °C; FT-IR (KBr, ν_{max}, cm^{-1}): 3244 (OH), 3037 (CH-arom), 2913 (CH-aliph), 1714 (CO), 1614 (C=N), 1552 (N=N);

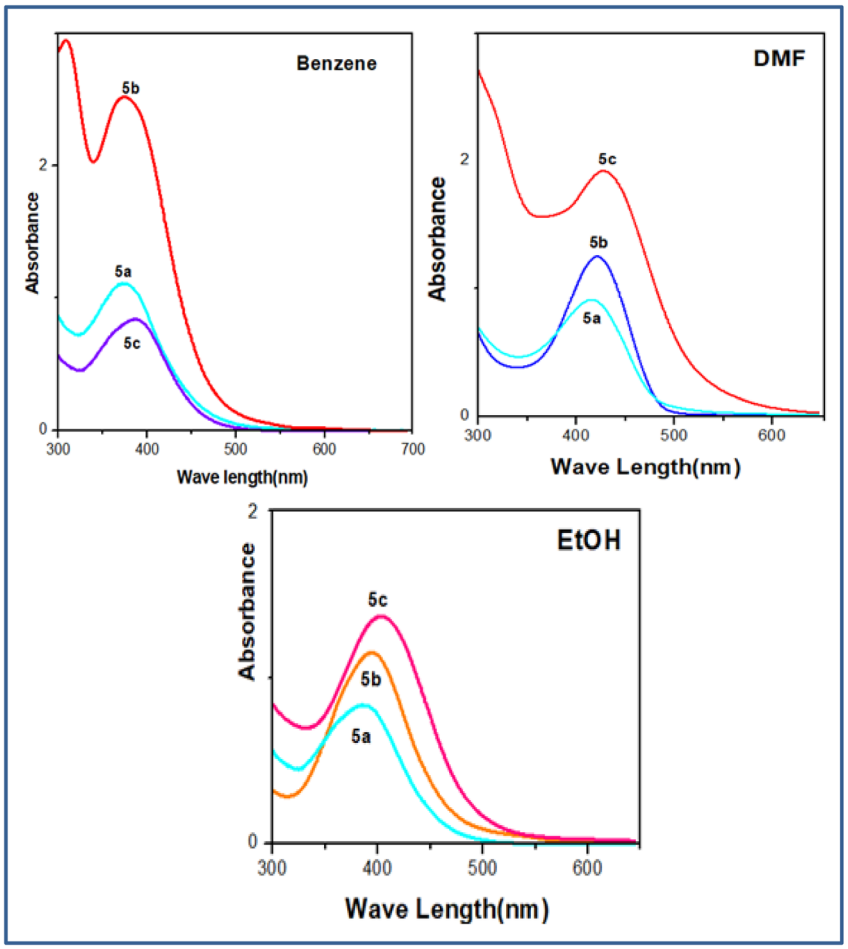

Fig. 4 Dyes **5a–c** absorption spectra in different solvents.

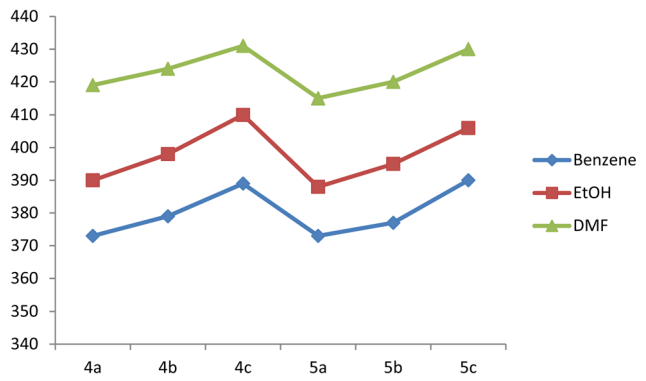

Fig. 5 Effect of solvent on absorption spectra of compound **4a–c** and **5a–c**.

^{1}H-NMR (400 MHz, DMSO-d_6, δ, ppm): 6.70–8.43 (m, 19H, Ar-H), 6.51 (s, 1H, OH), 2.33 (s, 3H, CH_3); ^{13}C NMR (100 MHz, DMSO-d_6, δ, ppm): 187.15 (C=N Schiff base), 167.78 (C=N quinazolinone), 156.40 (C=O quinazolinone), 117.33–148.11 (Ar-C), 13.77 (CH_3); MS (EI) m/z [M^+ + 2] calcd for $C_{32}H_{23}N_5O_2$: 509.57, found: 509.94; anal. calcd for $C_{32}H_{23}N_5O_2$ (509.57): C, 75.43%; H, 4.55%; N, 13.74%. Found: C, 77.13%; H, 4.35%; N, 13.56%.

Electronic spectral studies. At a molar concentration of 1×10^{-5} mol L^{-1} in ethanol, benzene, and dimethylformamide (DMF), the electronic spectra of the quinazolinone dyes **4a–c** and **5a–c** were examined in the ultraviolet area.

Dyeing procedure of polyester fabric. Dyeing of polyester fabric was carried out using a procedure reported in the literature[45,46] as illustrated in Fig. 2 and was described in the SI (Section S2).

Measurement of the dyeing properties

Fastness properties. The fastness properties of the dyed fabrics were evaluated in the SI (Section S3).

Colorimetric analysis. Colorimetric education is offered in the SI file (Section S4).

Exhaustion and fixation study. The percentage dye bath exhaustion and fixation of the dyed fabric are discussed in the SI file (Sections S5 and S6).

Ultraviolet protective factor (UPF). UPF analysis of the blend fabrics was carried out and is discussed in the SI file (Sections S7).[47]

Molecular docking *in silico* simulations. The molecular docking software Molegro Virtual Docker was used to study the biochemical interactions between synthesized compounds **5b**

Table 2 Shade of fabric samples dyed with **4a–c** at 2% owf level

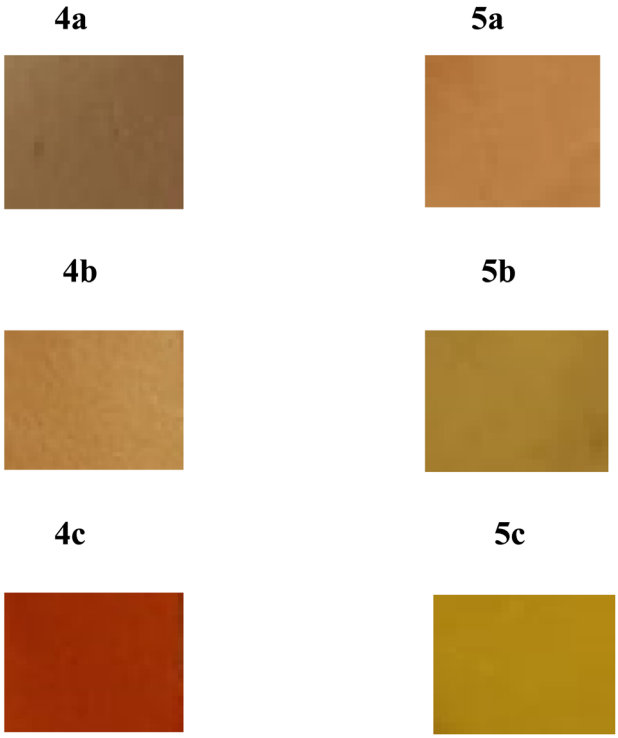

and **5c** against the DNA gyrase protein. *E. coli* DNA gyrase crystal structure (PDB ID: 5L3J) was downloaded from the Protein Data Bank server. To increase effectiveness, the target proteins were kept free of co-crystallized ligands, heteroatoms, and water molecules. Using ChemDraw Ultra 8.0, the synthesized analogs' 2D structures were created in cdx format, which was afterward transformed into motif files for 3D structures and energy minimization using the (MM2) force field. Molegro Virtual Docker examined the interactions between target proteins and ligands. The Piecewise Linear Potential (PLP) algorithm is the scoring function in computational screening. The MolDock simplex evolution search algorithm operates with a grid resolution of 0.30 Å. Among the ten poses generated, they were arranged based on their MolDock Scores, and for further analysis, the pose with the lowest Rerank Score was chosen. Discovery Studio 3.5 was used to visualize the intermolecular interactions.[48] The online tool Swiss ADME was used for estimating the ADMET features.[49]

Antimicrobial activities

Microorganisms' origin. Tanta University Hospital's clinical laboratory kindly contributed to the clinical strains used in this investigation. The acquired pathogenic microorganisms comprised four strains of multidrug-resistant Gram-positive and Gram-negative bacteria and two species of unicellular pathogenic fungi. Specifically, the bacterial strains utilized in the study were *Escherichia coli*, *Pseudomonas aeruginosa*, *Staphylococcus aureus*, and *Bacillus subtilis*, while the fungal strains comprised *Candida albicans* and *Aspergillus flavus*.

Evaluation of the antimicrobial action of the synthesized compounds. After dissolving each of the produced compounds in DMSO, a solution with a concentration of 1 mg mL^{-1} was created. Standard-sized (5 cm) Whatman filter paper discs were cut and autoclave sterilized. The petri dishes with nutritional agar media (agar (20 g), beef extract (3 g), and peptone (5 g)) seeded with the various bacterial and fungal strains were aseptically filled with paper discs soaked in the appropriate concentration of the complex solution. After 24 hours of incubation at 36 °C, the inhibitory zones in the petri dishes were measured. Three duplicates of each treatment were made. The same method as previously described was used to record the antibacterial activity of the common standard antibiotic levofloxacin, ampicillin and the antifungal Clotrimazole at the same concentration and solvents. The following formula was used to determine the complex's percentage activity index:

$$\%\ \text{activity index} = \frac{\text{zone of inhibition by test compound (diameter)}}{\text{zone of inhibition by standand (diameter)}} \times 100$$

The minimum inhibitory concentration (MIC) was investigated. First, bacterial or fungal strains were put in 10 mL of nutrient soup and left to grow overnight at 30 °C. Test tubes with 9.5 mL of 10× diluted nutrition soup were cleaned and ready to use. A 0.5 mL sample of the bacteria grown overnight was put into each tube. The chosen bioactive chemicals were put into the tubes, and then the synthesized compounds were

kept at 30 °C in a shaking incubator. The number of viable cells, shown as CFU mL^{-1}, was found after 24 hours.

Results and discussion

The preliminary compounds **2** and/or **3** were manufactured according to ref. 25. As seen in Schemes 1–3, the corresponding compounds **4a–c** and **5a–c** were produced in good yield by coupling different phenol derivatives with compound **2**, **3**'s diazonium salts in NaOH. The structures of dyes **4a–c** and **5a–c** were identified through elemental analyses, mass spectrometry, FT-IR, 1H, and ^{13}C NMR. The FT-IR spectra of dyes **4a–c** and **5a–c** revealed distinct bands for (NH_2) at 3325–3460 cm^{-1}, for the OH at 3215–3254 cm^{-1}, and for the azo group (N═N) bending vibration at 1525–1575 cm^{-1}. Furthermore, an absorption band at 1590–1654 cm^{-1} resulting from the quinazolinone moiety's C═N stretching vibration and a strong band at 1725–1755 cm^{-1} corresponding to the C═O group were noted. The ^1H NMR spectra of dyes **4a–c** displayed a singlet signal at δ 2.34–2.43 ppm that was attributed to a CH_3 proton, a broad peak at δ 4.99–6.55 ppm that corresponded to OH protons, and a broad peak at δ 8.69–8.96 ppm, which was caused by NH_2 protons that were exchangeable with D_2O. The ^1H NMR spectra of dyes **5a–c** revealed a singlet signal credited to the CH_3 proton at δ 2.19–2.37 ppm and a broad peak at δ 4.96–6.55 ppm, which was responsible for OH protons, and a broad peak at δ 10.26–10.28 ppm, for NH_2 protons, which were exchangeable with D_2O. The ^{13}C NMR spectral data of dyes **4a–c** and **5a–c** were consistent with the structures that were anticipated, and the mass spectra established the molecular weights that were anticipated (see SI section (Fig. S1–S18)).

Spectroscopic characteristics related to visible absorption of dyes 4a–5c

Due to their increased polarity, predominantly in the excited state, azo disperse dyes based on heterocyclic display enhanced bathochromic impact compared to their benzenoid analogs and exhibit greater effects of solvatochromic.[50,51] Absorption spectra of the azo dyes derived from on quinazolinone derivatives were documented in numerous solvents as the polar protic solvent (ethanol), the dipolar aprotic solvent (DMF), and the nonpolar solvent (benzene) were utilized to record the electronic absorption spectra of dyes **4a–d** at room temperature and measure the concentration at about 10–5 mol L^{-1}, and the results are brief in Table 1, Fig. 3 and 4. The characteristics of the diazo and coupling components determine the color of these azo dyes. These dyes' electronic spectra showed an absorption band in the following regions: 373–390 nm for benzene, 390–410 nm for ethanol, and 415–431 nm for DMF. The azo groups, phenyl, and quinazolinone heterocycles are attributed to a transition of π–π* type, which was caused by electronic changes that affect the conjugate system.

Solvent effect on the absorption spectra

When identifying the azo dyes in ethanol and DMF, bathochromic shifts of the visible absorption band were also found

Table 3 Estimation of synthetic dyes' fastness characteristics on polyester textiles[a]

Dyes no.	Washing fastness			Rubbing fastness		Perspiration fastness						Sublimation		Light fastness
						Acidic			Alkaline					
	Alt.	St.*	St.**	Dry	Wet	Alt.	St.*	St.**	Alt.	St.*	St.**	210	180	
4a	4	4	4	4–5	4	4	4	4	4	4	4	4	4	4–5
4b	4	4	4	4–5	4	4	4	4	4	4	4	4–5	4–5	4–5
4c	4	4	4	4–5	4	4	4	4	4	4	4	4	4	5–6
5a	4	4	4	4–5	4	4	4	4	4	4	4	4	4	4–5
5b	4	4	4	4–5	4	4	4	4	4	4	4	4	4	4–5
5c	4	4	4	4–5	4	4	4	4	4	4	4	4–5	4–5	5–6

[a] St.* Staining on cotton, St.** Staining on wool, Alt. Alteration in color rate for light fastness: 4–8 (acceptable), 1–3 (not acceptable); rate for different fastness – 5 (acceptable), 1–2 (not acceptable).

on the aprotic solvent > polar protic solvent > nonpolar solvent, as indicated in Table 1. The difference in λ_{max} was 25–21 nm. For a system where the excited state is more polar than the ground state, this is expected.[52] Since most interactions between solutes and solvents are caused by hydrogen bonding, the strong hydrogen bonding between the ethanolic hydrogen and the nitrogen centers may explain why ethanol has a lower influence on the transition energy as a polar protic solvent. All dyes showed the maximum sensitivity in this particular solvent because DMF is polar and alkaline (Fig. 5).

Substituent influence on the absorption spectra

The dye's absorption properties are prejudiced by the presence of electron-donating and electron-attracting groups at appropriate positions within the coupled ring. Table 1 demonstrates that azo groups in dyes **4c** (389–431) and **5c** (390–430) that have an electron-accepting hydroxyl and naphthyl group attached to them cause a bathochromic shift in all solvents regarding electron-donating NH_2 groups. Strong electron-accepting groups in these dyes contribute to the conjugated system's heightened delocalization, which helps to clarify this behavior. The absorption maximum of dyes in series, **4a, b** and **5a, b** is determined by the substituent's position in the benzene ring, where the *o*-position results in a longer bathochromic shift than the *m*-position.

Dyeing process on polyester (PE) fabrics

With a high-pressure temperature method (130 °C) and a shade of 2%, the recently synthesized disperse dyes **4a–5c** were used to dye the polyester fabrics. To acquire the anticipated color and quality, dispersing azo dyes is a complicated dyeing process that requires careful attention to detail. The auxochrome X's characteristics and position within the arylazo portion, which permeated the fibers, are accountable for the noticed variations in the dyed polyester samples' color shades. It is noted that a similar substituent exhibits dissimilarity in shade at several positions within the phenyl moiety, leading to outstandingly different shades depending on its placement. Conversely, the fiber's color shade altered strikingly when the change-like substituents were added (Table 2).

Dyeing properties on polyester fabrics

Assessment of the fastness property. A dyed fiber is said to be colored fast if it retains its color through exposure to light, rubbing, washing, and other environmental conditions. The type of dye used, the dyeing process, the type of fiber, and the environment the fiber is exposed to all affect how color-fast the fiber is. For dyed fabrics to last a long time and be resistant to fading and discoloration, high color fastness is vital. The dye-fiber affinity and adequate dye diffusion into the textiles are the reasons why the polyester fibers that have been dyed with **4a–5c** display very good fastness to fading and washing (**4**). The hydrophobic group (C═O) that the dyes contain prevents them from returning to the washing solution bath. Additionally, after washing, a remarkable color leveling was achieved, demonstrating the high energy of the dye–fiber and dye–dye interaction, regardless of pH level, the majority of dyed fabrics received very good ratings (**4**) for perspiration fastness, indicating that pH level does not affect the dyed samples' sensitivity. This may be clarified by the dyes' natural resistance to deterioration in both basic and acidic environments. The high rate of dye molecule absorption into the materials is responsible for the excellent rubbing fastness values (**4–5**) (both wet and dry). The good to very good sublimation fastness properties of all the synthesized dyes contributed to the manufacture of a high molecular absorption coefficient rather than just a large dye movement at elevated temperatures. The artificial dyes **4a** and **b**, and **5a** and **b** exhibited good light fastness properties (**4–5**), whereas dyes **4c** and **5c** showed very good light fastness properties (**5–6**). This is because dyes that contain electron-donating groups, such as amino groups, are more likely to undergo photochemical reactions and be more susceptible to photodegradation. It has been noted that the light fastness of azo dyes can be improved by electron-accepting groups. As indicated in Table 3, this observation lends credence to the idea that azo dyes with substituents that withdraw electrons (naphthalene moiety) on their diazo components are less susceptible to photofading.[53]

Color assessment. Because chromophores are incorporated into the structures of dyes **4a–5c**, they established good color depth and leveling properties after being applied to polyester fabrics (Table 4). The color coordinates demonstrate that the dyes display evenness, good color depth, brightness, and, when applied to polyester fabrics. By comparing the L^* values, where negative and positive values denote darkness and lightness, respectively, it was possible to determine how dark or light the dyes were on polyester fabrics. Dye **4a–5c** had L^* values ranging from 64.69 to 72.35, as Table 4 illustrates. According to Table 4, **4a** is the dye that had the greatest effect on the brightness value (L^*) of the PE samples. The dye's color hues were found to shift to a yellowish direction on the yellow-blue axis and a reddish direction on the red-green axis, respectively, in all dyed fabrics **4a–c** and **5a–c**, with a^* and b^* values that are positive. From the visual observations of the colored fabrics, these findings show that the dyes under investigation had good leveling qualities and good affinity.

Visual assessment of color uniformity is measured quantitatively by measuring the color strength (K/S) at different random points on each dyed sample for all dyes. Then CV% (variation coefficient) is calculated as the standard numerical indicator of color levelness or uniformity and the data are

Table 4 Optical measurements of all synthetic dyes on polyester fabrics

Dye no.	L^*	a^*	b^*	% E	% F
4a	70.03	12.7	23.16	78	81
4b	64.69	18.81	14.19	79	75
4c	67.71	18.19	53.97	89	82
5a	72.35	12.66	45.02	85	79
5b	68.98	19.1	29.49	87	80
5c	67.94	17.59	38.39	92	84

Table 5 Color strength (K/S) values at maximum wavelength values of dyes **4a–c**, and **5a–c** at different random locations

Dye	K/S (1)	K/S (2)	K/S (3)	K/S (4)	K/S (5)
4a	2.11	2.43	2.31	2.52	2.47
4b	2.97	3.11	2.99	2.86	2.75
4c	2.23	2.11	2.36	2.09	2.38
5a	2.98	3.34	2.88	3.11	2.77
5b	2.01	1.99	2.19	2.21	2.08
5c	2.24	2.26	2.18	2.35	2.31

Table 6 Coefficient of variation (CV%)

	4a	**4b**	**4c**	**5a**	**5b**	**5c**
Mean	2.37	2.94	2.23	3.02	2.10	2.27
Std deviation	0.15	0.12	0.12	0.20	0.09	0.06
CV%	6.19	4.16	5.42	6.53	4.31	2.58

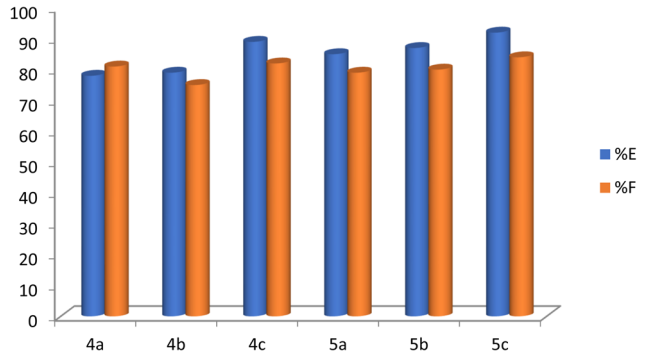

Fig. 6 Percentages of polyester fabric dye fixation and exhaustion.

tabulated in Tables 5 and 6. From the CV% (variation coefficient) value we concluded that a lower value for CV% indicates better color uniformity or levelness (Tables 5 and 6).

Dye exhaustion and fixation. Table 4 and Fig. 6 present the exhaustion and fixation efficiency (% *E*, % *F*) values of dyes **4a–c** and **5a–c** on polyester samples. It reveals that the substituent's characteristics and position in the aryl moiety are somewhat connected with the exhaustion efficiency and fixation values. Dyes **4c** and **5c** have excellent dye *E*% and % *F*, while the remaining dyes have very good dye *E*% and % *F*, as seen by the dyed fabrics' photofading. This proposes that exhaustion values are meaningfully influenced by the type of substituent. This could be due to the structure of the fabric as well as the substituent's X characteristics and position. The capability of the dye to enter and stay inside the fiber to the appropriate depth can also be aided by and influenced by substitutes.

Effect of pH on color strength. The pH of the dye bath is one of the most crucial factors to consider when determining the ideal dyeing conditions for dispersion of dye on polyester textiles. To investigate the color strength of dyed polyester in terms of K/S on polyester fabrics, dispersion dyes were applied to polyester fabrics at a high temperature without the use of carriers and at different dyebath pH ranges from 3 to 11. The

Table 7 Effect of pH on the color strength (K/S) of polyester fabric dyed with **4a–c**

	K/S				
Dye no.	pH 3	pH 5	pH 7	pH 9	pH 11
4a	0.88	1.91	2.88	1.37	0.8
4b	3.6	2.84	2.54	2.09	2
4c	1.01	2.18	3.07	2.13	1.86
5a	5.2	2.83	2.78	2.08	1.52
5b	1.68	1.81	1.27	1.19	1.01
5c	2.39	2.1	1.78	1.68	1.43

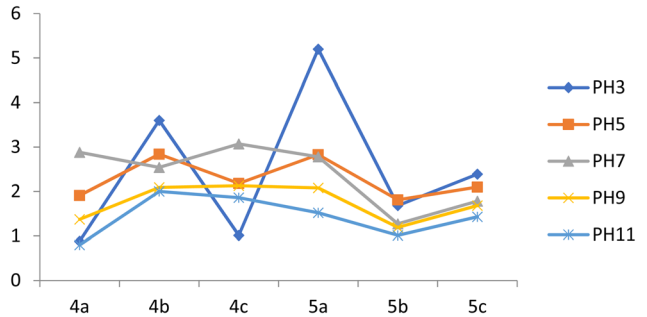

Fig. 7 Effect of dyeing pH on (K/S) values of polyester fabric.

impact of dyeing pH on color strength is shown in Table 7 and Fig. 7. The color strength (K/S) values of dyes **5a**, **5c**, and **4b** are higher at pH 3, whereas dye **5b** produces the highest K/S values at pH 5. At a higher pH 7, dye **4a** gives polyester fabrics a better color. Additionally, the dye uptake value at pH 9 is lower than at pH neutral or acidic. The advanced aggregation of dyes resulting from their higher molecular weight can be attributed to the effect of dye bath pH on color strength value.

Effect of the dyeing time on the color strength. The dyeing process involves diffusion, dye fabric fixing, and surface adsorption. When the dyeing process reaches an equilibrium stage for a reaction period, the sorption and desorption equilibrium is reached at that exact point.[54]

On the other hand, longer dyeing times at higher temperatures would endorse additional effective dye desorption. Table 8 and Fig. 8 illustrates the characteristics of dyeing colors over time. The results showed that as dyeing times increased, so did the amount of dye absorb on fabrics. Because of its high

Table 8 Effect of dyeing time on the color strength (K/S) values

	K/S			
Dye no.	15 min	30 min	45 min	60 min
4a	0.9	1.4	1.42	2.08
4b	2.14	2.24	2.66	3.18
4c	0.68	1.02	1.56	2.01
5a	2.04	3.72	5.12	5.96
5b	1.31	1.58	2.31	2.66
5c	1.84	4.94	12	12.67

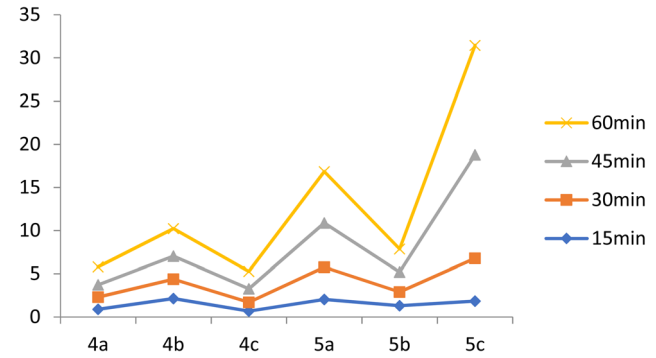

Fig. 8 Effect of dyeing time on (K/S) values of polyester fabric.

Table 9 Effect of pH on the color strength (K/S) of polyester fabric dyed with **4a–c**, and **5a–c**

	K/S			
Dye no.	0.5%	1%	2%	3%
4a	0.6	0.7	1	1.06
4b	0.91	2.06	2.26	3.14
4c	0.87	0.96	1.32	1.58
5a	1.08	1.24	1.98	2.17
5b	1.81	2.63	2.98	4.76
5c	2.21	3.92	4.62	6.94

substantivity, the proportion of dye exhaustion rose expressively in the first 60 minutes of dyeing and then gradually increased in the final 60 minutes. Moreover, it was revealed that as the dyeing processes proceeded, the dyes' total fixation yield enlarged, yielding higher color strength values.

Effect of dye concentration on color strength. For the dyes **4a–c** and **5a–c**, a relationship between the K/S value at the λ_{max} and the dye quantity was recognized, as demonstrated in Table 9 and Fig. 9. Deeper shades are fashioned as a result of increased dye adsorption and an increase in color strength (K/S) with a dye concentration increase from 0.5 to 3.0% (owf). The rate at which dye disperses from the dyebath solution onto the surface of the fiber ultimately rises as a result of the dye concentration in the dyebath increasing and the concentration gradient increasing. The results indicate that when the dye concentration was altered from 0.5 to 3%, the K/S value of the dyed fabric progressively increased. To accomplish the greatest exhaustion, a dye concentration of 3% owf was consequently found.

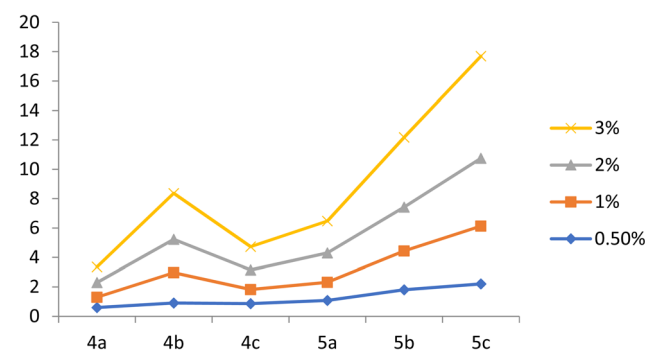

Fig. 9 Effect of dye concentration on (K/S) values of polyester fabric.

Ultraviolet protection factor (UPF)

Numerous methods exist for protecting against harmful ultraviolet radiation (UVR), including the use of sunscreen, chemical laundry additives, regular clothing, and photoprotective clothing. Though research has demonstrated that prolonged use of sunscreen can have major neurological, endocrine, and developmental consequences, it is still a widely used sun protection technique. Chemical laundry additives have been promoted as a way to reflect or absorb UV radiation, but there is currently no information on their effectiveness in tests, and skin contact with these chemicals may be hazardous. Sun protection is imparted by dyes, weave patterns, and textile materials on all clothing, whether it is sun-protective or not. On the garment protection factor (GPF) and ultraviolet protection factor (UPF) scales; however, photoprotective apparel is typically rated as being more protective. The best approach to protect from the sun with the least amount of risk is probably to wear photoprotective clothing and apply sunscreen to any exposed skin. To learn more about the subject, though, more research is required.[55] UVR can be further divided into ultraviolet A (UVA), ultraviolet B (UVB), and ultraviolet C (UVC) types according to their wavelengths. While UVB rays can burn skin and UVA rays can hasten the aging process of skin, UVC rays are absorbed by Earth's atmosphere and do not penetrate. Sunscreen and

Table 10 Ultraviolet protection factor rating

			Effective UV-R transmission (%)	
Dyes no.	UPF range	Protection category	UV-B	UV-A
4a	53.59	Excellent	0.01	0.14
4b	48.78	Excellent	0.03	0.16
4c	56.22	Excellent	0.02	0.12
5a	50.12	Excellent	0.05	0.15
5b	49.66	Excellent	0.04	0.10
5c	51.35	Excellent	0.01	0.18

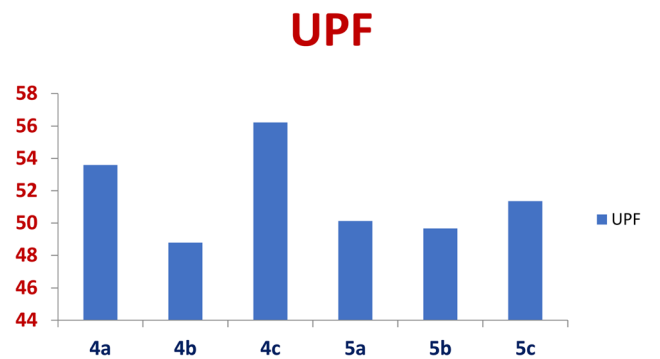

Fig. 10 UPF blocking (%).

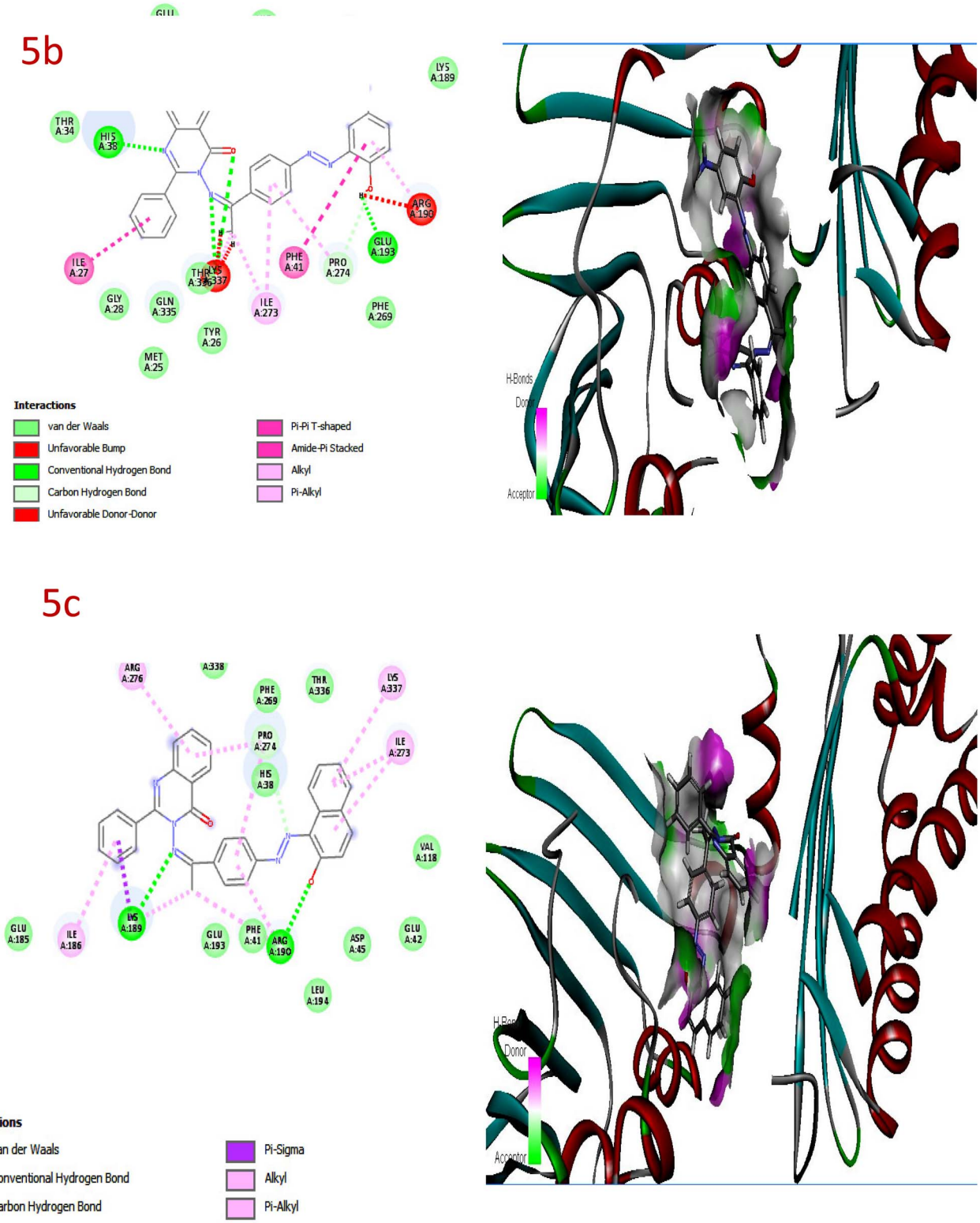

Fig. 11 Molecular docking interaction of compounds **5b** and **5c** against bacterial DNA gyrase.

clothing with UV protection are two contemporary ways to reduce the harm that UV radiation can cause.[56] Three groups of textile products are distinguished by their UPF rating: UPF range (15–24) good UV protection, UPF range (25–39) very good UV protection, and UPF range (40–50+) excellent UV protection. For every new synthetic dye, the UPF results for cotton/polyester fabrics were displayed in Table 10 and Fig. 10. Depending on the UPF values, which ranged from 48.78 to 56.22 and represent

the transmittance percentage in the range of ≤2.5% (blocking approximately 100% of the UV radiation), dyed polyester fabrics **4a–c** and **5a–c** showed an excellent UPF rating. Darker or more intensely colored dyes absorb more UV radiation, leading to higher Ultraviolet Protection Factor (UPF) values. The electronic properties of the dye which contain electron-donating groups as amino, and hydroxyl groups influence this absorption capacity.[57] From the data we showed that the UV protection offered by dyes based on quinazolinone moieties which absorb UV radiation due to their conjugated systems and electron-rich aromatic and/or heterocyclic structures, which allow them to strongly absorb and dissipate UV energy, protecting the fabrics from radiation damage. The conjugated double bonds and heteroatoms in the quinazolinone structure facilitate electronic transitions that prevent UV light penetration.

In silico docking investigations

Since molecular docking is an effective method for rapidly and accurately predicting the biomolecular conformations and binding energies of protein-ligand complexes, it has been widely used in the development of new medications. Bacteria have numerous defenses against foreign invaders, including a widely distributed bacteriophage defensive system called CBASS (cyclic oligonucleotide-based anti-phage signaling system). A cGAS/DncV-like nucleotidyl transferase in CBASS systems responds to infection by producing cyclic di- or trinucleotide second messengers. Through abortive infection, these molecules mediate bacteriophage immunity by activating a variety of effectors. To determine the binding mode of interactions and to create the ideal conformation of the most active molecule (**5b**) and the least active one (**5c**), molecular docking analysis was used. While compound **5c** only has a low antibacterial efficacy, compound 5b has a high antibacterial potency and may also operate as an antibiotic, as shown by the results in Fig. 11 and Table 11. Furthermore, compound **5b** inhibited bacterial DNA gyrase with a binding score of −10.32 kcal mol^{-1} with interactions like van der Waals, hydrogen bond, Pi–Pi T-shaped, alkyl, and pi–alkyl, according to the experimental results and molecular docking studies. However, compound **5c** showed less binding affinity with a binding score of −7.86 kcal mol^{-1} with interaction as van der Waals, hydrogen bond, alkyl, and pi–alkyl as shown in Fig. 11 and Table 11. We concluded that the antibacterial impact of the synthesized compounds, particularly compound **5b**, is due to their ability to bind and restrain DNA gyrase of the bacteria, which is responsible for bacterial DNA topology, transcription, and replication.[58]

Table 11 Molecular docking interaction of compounds **5b** and **5c** against bacterial DNA gyrase

	DNA gyrase	
Compounds	Docking score (ΔG_{bind})	Docked complex (amino acid–ligand) interactions
5b	−10.32	**van der Waals**
		THPA336
		Hydrogen bond
		GLUA193
		HISA38
		PROA274
		Pi–Pi T-shaped
		PHEA41
		ILEA27
		Alkyl and Pi–alkyl
		ILEA273
		VALA118
5c	−7.86	**van der Waals**
		PHEA41
		HISA38
		Hydrogen bond
		LYSA189
		ARGA190
		PROA274
		Alkyl and Pi–alkyl
		LYSA337
		ILEA273
		ILEA186
		ARGA276

ADMET features

The inherent activity of a drug is not the only determinant of its efficacy following administration. A drug must navigate multiple barriers to get at its target spot without incurring metabolic degradation. Therefore, evaluating the ADMET profile of drug candidates is essential early in drug discovery to improve the probability of clinical success during development. Currently, *in silico* approaches are widely employed for the rapid assessment of safety, pharmacokinetics, and toxicological characteristics of new compounds prior to undertaking expensive experimental processes.[48]

The drug-like characteristics and bioavailability of compound **5b** and standard drugs were determined and depicted in Table 12 and Fig. 12. It demonstrated exceptional permeability and adequate oral bioavailability, as evidenced by their respective total polar surface area (TPSA) values of 118.22 $Å^2$. Moreover, the elevated log *p* values observed in compound **5c** represent intentional and strategic design features as the disruption of protein–protein interactions (PPIs) requires compounds with sufficient lipophilicity to engage effectively with the large hydrophobic interface's characteristic of this challenging target class. Additionally, it demonstrated flexibility by displaying rotatable bonds between 0 and 10. Because itis HBA and HBD values fell within the satisfied range, it was more soluble in cellular membranes. According to Tables 12, it is log *p* values below 6 have good lipophilicity features. Additionally, our product met the ADMET criteria with higher % HIA ratings, indicating that it could be more effectively absorbed by the human gut. The anticipated blood–brain barrier (BBB) permeability value indicate that the compounds are improbable to traverse the BBB, which corresponds with their intended peripheral therapeutic use and reduces central nervous system-related adverse effects.[48] Because the tested compound doesn't pass through the BBB, itis safety profile for the central nervous system (CNS) is excellent. In conclusion, all of the AME'S toxicity

Table 12 ADMET assets

	Molecular weight (g mol^{-1})	Blood–brain barrier (BBB)	% Human intestinal absorption (HIA^{+})	TPSA A^2	Log *p*	nHA	nHD	*N* rotatable	AMES toxicity	Carcinogenicity
5b	474.180	NO	78.22	118.22	4.90	8	3	5	Nontoxic	Noncarcinogenic
Ampicillin	349.11	NO	76.55	112.73	1.52	7	4	5	Nontoxic	Noncarcinogenic
Clotrimazole	344.11	NO	77.32	17.82	5.25	2	0	4	Nontoxic	Noncarcinogenic
Levofloxacin	361.140	NO	75.82	75.01	0.25	7	1	2	Nontoxic	Noncarcinogenic

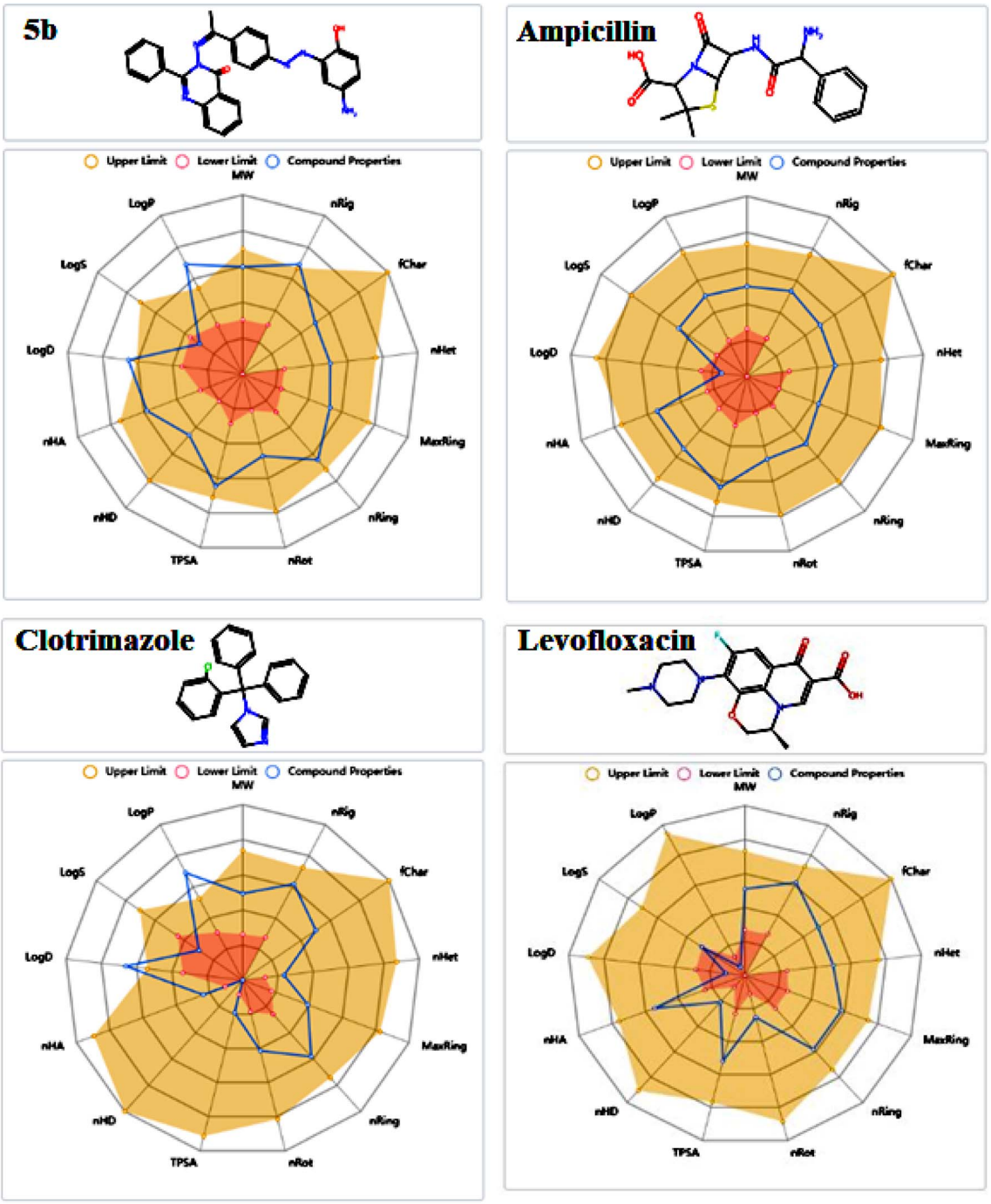

Fig. 12 Bioavailability radar plot for compound **5b** and standard drugs.

Table 13 Synthesized dyes' inhibitory zone diameters (mm) against various bacteria and fungi

	Diameter of inhibition zone (mm)					
Compounds	*E. coli*	*P. aeruginosa*	*S. aureus*	*B. subtilis*	*C. albicans*	*A. flavus*
4a	14	14	18	17	14	16
4b	11	10	12	13	12	13
4c	13	15	16	14	16	17
5a	14	16	15	18	18	17
5b	10	9	11	10	14	11
5c	15	17	18	19	21	20
Levofloxacin	25	22	21	24	NA	NA
Ampicillin	25	23	24	23	NA	NA
Clotrimazole	NA	NA	NA	NA	27	25

Table 14 Minimum inhibitory concentration (MIC) of the newly synthesized dyes **4a–5c** and antibiotics (μM)

	Gram-negative bacteria		Gram-positive bacteria		Fungi	
Compounds no.	*E. coli*	*P. aeruginosa*	*S. aureus*	*B. subtilis*	*C. albicans*	*A. flavus*
4a	49	52	61	55	57	57
4b	95	98	99	87	89	96
4c	52	49	55	48	40	43
5a	44	45	49	58	48	54
5b	94	90	94	89	84	87
5c	35	39	43	47	40	42
Levofloxacin	20	12	17	15	NA	NA
Ampicillin	10	10	25	10	NA	NA
Clotrimazole	NA	NA	NA	NA	18	21

and carcinogenicity test results were negative, proving that it is safe.

Antimicrobial activity

Bacterial infections are a chief source of mortality and a threat to humankind. There is a persistent requirement to progress to more potent antibacterials because drug resistance, principally multidrug resistance resulting from dissimilar defensive mechanisms in bacteria, is the primary source of chemotherapy disappointment. The quinazoline and quinazolinone frameworks have drawn a lot of awareness because of their extensive variety of therapeutic uses. Precisely, quinazoline/quinazolinone hybrids are operative scaffolds for the discovery of new antibacterial agents and have the potential to exhibit antibacterial activity through a diversity of mechanisms.[59] The *in vitro* antimicrobial activities of the produced dyes **4a–c** and **5a–c** were appraised against a panel of two-gram positive bacteria (*S. aureus*, *B. subtilis*), as well as two Gram-negative bacteria (*P. aeuroginosa*,*E. coli*). Two fungi (*C. albicans* and *A. flavus*) were used to examine the compounds' antifungal activities; the recently fashioned compounds' inhibition zone (IZ) diameter was distinguished from that of the reference drug, levofloxacin, ampicillin, and clotrimazole. The attained results are shown in Table 13.

Commonly, dyes **4a**, **4c**, **5a**, and **5c** showed very good activities for Gram-negative bacteria (*E. coli*), while dyes **4b** and **5b** presented moderate activities with the reference antibiotic levofloxacin and ampicillin. When related to the reference drug ampicillin, dyes **4a**, **4c**, **5a**, and **5c** demonstrated extremely good activities for Gram-positive bacteria (*S. aureus*), but dyes **4b** and **5b** showed moderate activities. Dyes **4a**, **4c**, **5a**, and **5c** disclosed very good activities for Gram-negative bacteria (*B. subtilis*), while dyes **4b** and **5b** showed moderate activities. When compared to the reference medication Colitrimazole, dye **4b** displayed good activities against *C. albicans*, but all of the dyes established very good to excellent antifungal activity against *C. albicans*. Furthermore, when associated with the reference drug Colitrimazole, dyes **4a**, **4c**, **5a**, and **5c** exhibited very good activities, and dyes **4b** and **5b** disclosed good activities against *A. flavus*.

Bacteriostatic and fungistatic activity. The minimum inhibitory concentration (MIC) of manufactured derivatives **4a–5c** was evaluated against several microbial strains to establish their antimicrobial efficacy. A concentration nominated as MIC, with values expressed in μM, is one that, following spot subculture, displays no discernible growth.[60] Using broth microdilution, every generated compound's *in vitro* antibacterial activity was inspected. As standard drugs and positive controls, levofloxacin, ampicillin and clotrimazole were employed (Table 14). With MIC values of 35–61 μM against bacterial strains, the produced dyes **4a**, **4c**, **5a**, and **5c** showed the highest levels of activity when compared to ampicillin (MIC = 10–25 μM). Furthermore, with MIC values of 40 and 42 μM, respectively, dye **5c** established outstanding fungistatic ability against *C. albicans* and *C. flavus*. Additionally, the results

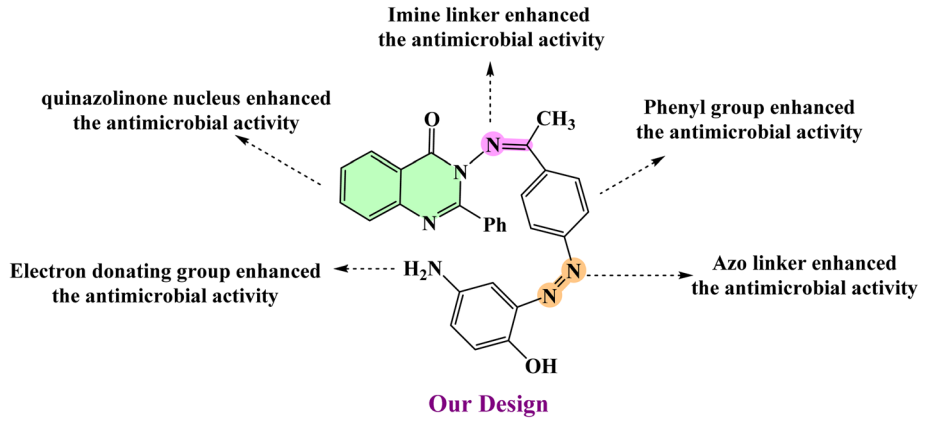

Fig. 13 Structure–activity relation of the novel synthesized azo quinazolinone.[10,49]

support the quinazolinone derivatives' promising antimicrobial activity, which can be heightened to have even superior antimicrobial activity.

Structure antimicrobial activity relationship (SAR). As described in Fig. 13, both *in silico* and *in vitro* studies demonstrated that compound **5b** was considered the most active compound due to the following reasons:

- The presence of a hetero nucleus (quinazolinone) and aromaticity (phenyl group) enhanced the antimicrobial activity against different types of Gram-positive bacteria, Gram-negative bacteria, and fungi by increasing the value of binding energy between the quinazolinone hetero atoms and the target protein *via* hydrogen bonding.
- The azo linker, imine linker, hydroxy group, and amino group in azo quinazolinone enhanced the binding with the target protein.

Conclusions

This work magnificently synthesized and dyed polyester fabric using an innovative biologically active quinazolinone dispersion dyes **4a–5c** in good yields. The structure of the synthetic dyes was ascertained by elemental and spectroscopic analyses. The greatest color strength and fastness (against rubbing, washing, light, sublimation, and perspiration) seemed to be accomplished at 130 °C, 60 minutes, and 3% dye concentration for all tinctures and 2% dye concentration for all dyes, according to the results of the dyeing procedures. The dyed samples demonstrated exceptional color consistency on polyester fabrics, with very good to excellent color fastness. The dyes disclosed a good to very good affinity for polyester fabrics with good to very good color depth and brightness. Because of the quinazolinone moiety, the synthesized dyes displayed excellent potential for antimicrobial functionality. This makes them promising compounds as safe, dispersible dyes for fabrics with antimicrobial effect. This manuscript opens admittance to a novel class of dyes to meet the textile industry's increasing necessity for dyes because the synthesis of these dyes is straightforward and reasonable, and they display dyeing properties identical to commercial dyes.

Author contributions

All authors contributed equally to the writing, review, and methodology.

Conflicts of interest

The authors have no relevant financial or non-financial interests to disclose.

Data availability

The data supporting this article have been included as part of the supplementary information (SI). Supplementary information is available. See DOI: **https://doi.org/10.1039/d5ra07614e**.

Acknowledgements

The authors extend their appreciation to the Deanship of Scientific Research, King Saud University for funding through Vice Deanship of Scientific Research Chairs (Drug Exploration and Development Chair), Project no. (MED-P-S-02-2025-06).

References

1 G. Muteeb, M. T. Rehman, M. Shahwan and M. Aatif, *J. Pharm.*, 2023, **16**, 1615.
2 M. A. Salam, M. Y. Al-Amin, M. T. Salam, J. S. Pawar, N. Akhter, A. A. Rabaan and M. A. A. Alqumber, *Healthcare*, 2023, **11**, 1946.
3 Z. Zhongbo and Q. Zhang, *Mater. Chem. Front.*, 2020, **4**(12), 419–3432.
4 G. Pei-Yang, Z. Wang and Q. Zhang, *J. Mater. Chem. B*, 2016, **4**(44), 7060–7074.
5 G. Pei-Yang, Z. Wang, G. Liu, H. Yao, Z. Wang, Y. Li, J. Zhu, S. Li and Q. Zhang, *Chem. Mater.*, 2017, **29**(10), 4172–4175.
6 W. Zilong, P. Gu, G. Liu, H. Yao, Y. Wu, Y. Li, G. Rakesh, J. Zhu, H. Fu and Q. Zhang, *Chem. Commun.*, 2017, **53**(55), 7772–7775.
7 A. A. Noser, M. Ezzat, Sh. G. Mahmoud, A. I. Selim and M. M. Salem, *Sci. Rep.*, 2024, **14**(1), 11586.

8 M. EI-Hashash, M. S. Salem and S. A. M. Al-Mabrook, *Res. Chem. Intermed.*, 2018, **44**, 2545M.
9 B. Magesh, D. Keerthika, K. Bharathi, M. Premavathi, M. Vijayalakshmi and J. Lavanya, *Life Med.*, 2023, **11**, 1879.
10 A. A. Noser, A. A. El-Barbary, M. M. Salem, H. A. Abd El Salam and M. Shahien, *Sci. Rep.*, 2024, **14**(1), 3530.
11 A. H. Abdelmonsef, M. Omar, H. R. Rashdan, M. M. Taha and A. M. Abobakr, *RSC Adv.*, 2023, **13**(1), 292.
12 M. F. Zayed, *Sci. Pharm.*, 2023, **91**(2), 18.
13 P. S. Auti, G. George and A. T. RSC, *Adv*, 2020, **10**(68), 41353.
14 A. Z. Omar, M. G. Mohamed, E. A. Hamed, M. A El-atawy and J. Saudi, *Chem. Soc.*, 2023, **27**, 101594.
15 S. M H obaida, A. E. Abd-Almonuimb and A. J. Jarad, *Egypt. J. Chem.*, 2020, **63**(12), 4719.
16 K. Mezgebe and E. Mulugeta, *RSC Adv.*, 2022, **12**(40), 25932.
17 P. T. Tasli, Ç. K. Atay, T. Demirturk and T. Tilki, *J. Mol. Struct.*, 2020, **1201**, 127098.
18 N. Ahmed, S. A. Ibrahim, H. A. Abd El Salam, N. MA El-Ebiary, H. SA Mandour and J. Iran, *Chem. Soc.*, 2023, **20**(12), 2963–2976.
19 H. Gaffer and T. Khattab, *Egypt. J. Chem.*, 2017, **60**, 41.
20 A. Afnan Nasser, *SHIFAA*, 2024, **2024**, 1–17.
21 I. Akawu, I. Y. Magaji, A. O. Adeyi, E. P. Akabuogu and Y. Aminu, *Chem.Class. J.*, 2025, **9**(2), 642–659.
22 L. Z. Fekri, M. Kadivar-Kalmarzi and R. S. Varma, *PAC*, 2025, **45**(5), 926–995.
23 A. A. Al. Asseel and A. A. S. Al-Hamdani, *Bull. Chem. Soc.*, 2025, **39**(8), 1559–1578.
24 P. Udhayakumar, P. Kavina, T. Viswanathan and A. Lalitha, *New J. Chem.*, 2025, **49**(22), 9441–9451.
25 S. A. Ibrahim, A. I. Selim, A. M. Sakr, S. A. Mahmoud and A. A. Noser, *Fibers Polym.*, 2024, **25**, 1349.
26 A. M. El-badrawy, N. Nagy, E. Abdel-Latif and A. A. Fadda, *Biointerface Res. Appl. Chem.*, 2021, **11**(5), 12937.
27 T. Aysha, M. El-Sedik, S. Abd El Megied, H. Ibrahim, Y. Youssef and R. Hrdina, *Arab. J. Chem.*, 2019, **12**, 225.
28 O. V. Kovalchukova, M. A. Ryabov, P. V. Dorovatovskii, Y. V. Zubavichus, A. N. Utenyshev, D. N. Kuznetsov, O. V. Volyansky, V. K. Voronkova and V. N. Khrustalev, *Polyhedron*, 2017, **121**, 41.
29 H. A. Ahmed, M. A. El-Atawy, F. S. Alamro, N. S. Al-Kadhi, O. A. Alhaddad and A. Z. Omar, *Molecules*, 2022, **27**, 8980.
30 V. Patil, N. Sekar, V. S. Padalkar, J. Rajput, S. R. Patil and S. V. Patil, *J. Mol. Struct.*, 2020, **1199**, 126984.
31 S. Mabhai, M. Dolai, S. K. Dey, S. M. Choudhury, B. Das, S. Dey, A. Jana and D. R. Banerjee, *New J. Chem.*, 2022, **46**, 6885.
32 M. A. El-Apasery, M. A. Abdellatif and S. M. Ahmed, *Egypt. J. Chem.*, 2024, **67**(1), 371–374.
33 Z. Omar, A. M. Khamis, E. A. Hamed, S. K. El-Sadany, E. M. Abdel Rehim, M. E. Elba, M. G. Mohamed and M. A. El-Atawy, *Sci. Rep.*, 2023, **13**, 21554.
34 M. N. El-Nahass, E. A. Bakr, M. M. El-Gamil and S. A. Ibrahim, *Appl. Organomet. Chem.*, 2022, **36**, 665.
35 S. A. Ibrahim and H. F. Rizk, *Text. Res. J.*, 2022, **92**, 2849.
36 A. Prashant, G. George and A. T. Paul, *RSC Adv.*, 2020, **10**(68), 41353–41392.
37 A. Nawaf and J. Umm, *J. Umm Al-Qura Univ. Appll. Sci.*, 2023, **9**(3), 294–303.
38 B. Ronald, *JIMB*, 2009, **36**(6), 775–786.
39 E. El-Sayed, E. Abd El-Aziz, H. A. Othman and A. G. Hassab, *Egypt. J. Chem.*, 2024, **67**, 87–97.
40 A. Rehman, G. Shabir, M. Mansha, S. Manzoor, S. A. Khan and S. Ali, *J. Alloys Compd.*, 2025, **1037**, 182386.
41 U. H. Siddiqua, S. Ali, M. Iqbal and T. Hussain, *J. Mol. Liq.*, 2017, **241**, 839–844.
42 M. M. Aftan, M. A. Toma, A. H. Dalaf, E. Q. Abdullah and H. K. Salih, *Egypt. J. Chem.*, 2021, **64**(6), 2903–2911.
43 A. K. Augustine and J. O. Otutu, *Egypt. J. Chem.*, 2020, **63**(10), 3949–3959.
44 D. P. Chattopadhyay, *Handbook of Textile and Industrial Dyeing, Principles, Processes and Types of Dyes*, 2011, vol. 1, pp. 150–183.
45 H. F. Rizk, S. A. Ibrahim and M. A. El-Borai, *Arab. J. Chem.*, 2017, **10**(2), S3303.
46 J. O. Otutu and E. M. Efurhievwe, *J. Appl. Sci.*, 2013, **13**(6), 92.
47 S. k. Md Salauddin, A. Wasim, M. Rony, F. Jian and M. K. Shekh Md, *Polymers*, 2022, **14**, 4366.
48 N. Ahmed, M. M. Salem, E. M. ElSafty, M. H. Baren, A. I. Selim and H. SA Mandour, *RSC Adv.*, 2025, **15**(17), 13214–13224.
49 N. Ahmed, M. M. Salem, M. H. Baren, A. I. Selim and E. M. ElSafty, *Sci. Rep.*, 2024, **14**(1), 28859.
50 K. L. Georgiadou and E. G. Tsatsaroni, *Dyes. Pigm.*, 2002, **53**, 73e8.
51 P. F. Gordon and P. Gregory, *Organic Chemistry in Color*, Springer Science & Business Media, 2012.
52 U. H. Siddiquaa, S. Alia, M. Iqbalb and T. Hussain, *J. Mol. Liq.*, 2017, **241**, 839.
53 Z. Li, L. Zhao, Y. Bian, Y. Li, J. Qu and F. Song, *Curr. Top. Med. Chem.*, 2022, **22**(12), 2022.
54 A. Ezzat, M. B. I. Mohamed, A. M. Mahmoud, R. S. Farag, A. S. El-Tabl and A. Ragab, *J. Mol. Struct.*, 2022, **1251**, 132004.
55 J. T Lu and E. Ilyas, *Cureus*, 2022, **14**(7), e27333.
56 D. M. Parkin, D. Mesher and P. Sasieni, *Br. J. Cancer*, 2011, **105**, 66–69.
57 R. V. Mishra, C. W. Ghanavatkar and N. Sekar, *Spectrochim. Acta, Part A*, 2019, **223**, 117353.
58 R. Richard and A. Maxwell, *Crit. Rev. Biochem. Mol. Biol.*, 1991, **26**, 335–375.
59 A. Ragab, Y. A. Ammar, A. Ezzat, A. M. Mahmoud, M. Basseem, I. Mohamed, A. S. El-tabl and R. S. Farag, *Comput. Biol. Med.*, 2022, **145**, 105473.
60 J. L. Rodriguez-Tudela, F. Barchiesi, J. Bille, E. Chryssanthou, M. Cuenca-Estrella, D. Denning and J. P. Donnell, *CMI*, 2003, **9**(8), 1–8.